An EXAFS Investigation of Hg(II) Binding to Mercuric Reductase: Comparative Analysis of the Wild-Type Enzyme and a Mutant Enzyme Generated by Site-Directed Mutagenesis

Scott A. Raybuck,[†] Mark D. Distefano,[†] Boon-Keng Teo,[‡] William Orme-Johnson,[§] and Christopher T. Walsh*,[†]

Contribution from the Department of Biological Chemistry and Molecular Pharmacology, Harvard Medical School, 25 Shattuck Street, Boston, Massachusetts 02115, Department of Chemistry, University of Illinois at Chicago, Chicago, Illinois 60680, and Department of Chemistry, Massachusetts Institute of Technology, Cambridge, Massachusetts 02139.
Received May 22, 1989

Abstract: Bacterial mercuric ion reductase is a unique metal-detoxification biocatalyst in its ability to reduce toxic Hg(II) salts to Hg(0). The enzyme contains FAD, a reducible active-site disulfide (Cys_{135}, Cys_{140}), and a C-terminal pair of cysteines (Cys_{558}, Cys_{559}). Previous studies from this laboratory have shown by mutagenesis that all four cysteines are required for efficient Hg(II) reduction. To determine whether Hg(II) bound at the active site of the EH_2 form of the enzyme exists in bis-ligation or higher ligation (tris or tetrakis) to the indicated cysteine residues, we have conducted the first mercury EXAFS studies on both wild-type enzyme (Cys_{135}, Cys_{140}, Cys_{558}, Cys_{559} = CCCC) and a very low activity C-terminal double alanine mutant (Cys_{135}, Cys_{140}, Ala_{558}, Ala_{559} = CCAA) form of mercuric reductase. Stoichiometric titration of the wild-type or CCAA enzyme EH_2 form was achieved with either $Hg(CN)_2$ or $HgBr_2$, as monitored by quenching of the Cys_{140} thiolate–FAD charge-transfer-complex absorbance band as well as by alterations in FAD fluorescence. Hg EXAFS of these stoichiometric enzyme–Hg complexes revealed distances, ligand identification, and ligand number consistent with bis-thiol coordination in both the CCAA mutant (as anticipated) and also in the CCCC wild-type mercuric reductase. Implications for the catalytic mechanism are addressed.

Mercuric ion reductase is the key enzyme component in a multigenic bacterial system that senses mercury in its environment, transports the Hg(II) into the cell, and performs redox chemistry on the metal ion to reduce it to elemental Hg(0) and render it nontoxic. We are currently studying *mer* operons from both Gram-negative and Gram-positive bacteria as a paradigm of metal ion processing in nature, with the goal of elucidating the mechanism at the molecular level.[1]

Mercuric reductase catalyzes the two-electron reduction of Hg(II) to Hg(0) utilizing reduced nicotinamide by the reaction:

$$Hg(SR)_2 + NADPH + H^+ \rightarrow Hg(0) + NADP^+ + 2\ RSH$$

The enzyme from several bacterial chromosomal and transposon sources possesses a redox-active disulfide and FAD cofactor[2] similar to other disulfide oxidoreductases such as glutathione reductase.[3-5] Despite these structural similarities, mercuric reductase is unique in its ability to rapidly reduce and detoxify Hg(II). As the enzyme possesses two reducible groups (a redox-active disulfide spanning Cys_{135} and Cys_{140} and FAD), and protein can exist in three redox forms, E_{OX}, EH_2, and EH_4.[6] The E_{OX} form contains both a disulfide and an oxidized FAD, while the predominant EH_2 form possesses a dithiol group but retains the oxidized FAD. The EH_4 species possesses both Cys_{135} and Cys_{140} as dithiol and reduced flavin ($FADH_2$) moieties.

By a combination of kinetic, spectroscopic, and active-site-directed mutagenesis studies on the Tn501-encoded mercuric reductase, we have adduced evidence for participation of Cys_{135} and Cys_{140} in catalysis and for a bona fide reduced flavin ($FADH_2$) intermediate in catalysis.[7,8] Stopped-flow kinetic experiments have indicated that the EH_2–NADPH species is kinetically competent for Hg(II) reduction[9] while the EH_2 species is not,[10] emphasizing the requirement for a more reduced enzyme species than that typically employed by other members of the disulfide oxidoreductase family. In addition to the redox-active disulfide, all five mercuric reductases sequenced to date[11] also contain a pair of cysteines (Cys_{558} and Cys_{559} in the Tn501 enzyme[12]) that are close to the carboxyl terminus (Tn501 MerA has 561 residues per subunit) but are not present in glutathione reductases or other disulfide oxidoreductases. Mutagenesis of both Cys_{558} and Cys_{559} has revealed that they are essential for rapid catalytic turnover of Hg(II) to Hg(0).[13] The double mutant enzyme Ala_{558}, Ala_{559} has a rate of Hg(II) reduction only 10^{-3} that of wild type. Spectroscopic and chemical modification experiments using the wild-type enzyme as well as the above mutants have also suggested that the C-terminal cysteine pair is located close to the redox-active disulfide and FAD moieties.[14] Most recently, we have demonstrated that inactive mutant homodimers Ala_{135}, Ala_{140}, Cys_{558}, Cys_{559} or Cys_{135}, Cys_{140}, Ala_{558}, Ala_{559} can be reconstructed in vivo or in vitro into active heterodimers possessing one catalytically functional active site per dimer;[15] this latter result suggests that the mercuric reductase active site resides at the subunit interface of the enzyme dimer and involves Cys_{135} and Cys_{140} from one subunit and Cys_{558} and Cys_{559} from the other subunit. The above mutagenesis studies combined with the known avidity of Hg(II) for thiol ligands led to the proposal that the unique ability of

[†] Harvard Medical School.
[‡] University of Illinois at Chicago.
[§] Massachusetts Institute of Technology.

(1) Walsh, C.; Distefano, M.; Moore, M.; Shewchuk, L.; Verdine, G. *FASEB J.* **1988**, *2*, 124–130.
(2) Williams, C. H., Jr. *Enzymes (3rd Ed.)* **1976**, *13*, 89.
(3) Krauth-Siegel, R. L.; Blatterspiel, R.; Saleh, M.; Schiltz, E.; Schirmer, R. H.; Untucht-Grau, R. *Eur. J. Biochem.* **1982**, *121*, 259.
(4) Williams, C.; Arscott, L.; Schulz, G. *Proc. Natl. Acad. Sci. U.S.A.* **1982**, *79*, 2199–2201.
(5) Shames, S. L.; Fairlamb, A. H.; Cerami, A.; Walsh, C. *Biochemistry* **1986**, *25*, 3519–3526.
(6) Fox, B.; Walsh, C. *Biochemistry* **1983**, *22*, 4082–4088.
(7) Schultz, P.; Au, K.; Walsh, C. *Biochemistry* **1985**, *24*, 6840–6848.
(8) Distefano, M.; Au, K.; Walsh, C. *Biochemistry* **1989**, *28*, 1168–1183.
(9) Sahlman, L.; Lambier, A.-M.; Lindskog, S.; Dunford, H. *J. Biol. Chem.* **1984**, *259*, 12403–12408.
(10) Miller, S. M.; Massey, V.; Ballou, D.; Williams, C. H., Jr. *J. Biol. Chem.* **1986**, *261*, 8081–8084.
(11) Wang, Y.; Moore, M.; Levinson, H.; Silver, S.; Walsh, C.; Mahler, I. *J. Bacteriol.* **1989**, *171*, 83–92.
(12) Brown, N.; Ford, S.; Pridmore, R.; Fritzinger, D. *Biochemistry* **1983**, *22*, 4089–4095.
(13) Moore, M.; Walsh, C. *Biochemistry* **1989**, *28*, 1183–1194.
(14) Miller, S. M.; Moore, M.; Massey, V.; Williams, C. H., Jr.; Distefano, M.; Ballou, D.; Walsh, C. T. *Biochemistry* **1989**, *28*, 1194–1205.
(15) Distefano, M.; Moore, M.; Walsh, C. Manuscript in preparation.

0002-7863/90/1512-1983$02.50/0

mercuric ion reductases to catalytically process Hg(II) to Hg(0) may involve tridentate or tetradentate ligation of these four cysteinyl residues to enzyme-bound Hg(II) during the unique catalytic reduction cycle of mercuric reductase.[14]

To elucidate the Hg(II) coordination environment in mercuric reductase, we have employed extended X-ray absorption fine structure (EXAFS) spectroscopy. EXAFS has been used extensively to probe the structural environment of specific metals in metalloproteins, providing information on the type of ligand, metal–ligand bond distances, and coordination numbers.[16] Surprisingly little is known about the coordination chemistry of mercurated proteins, despite the widespread use of mercury enzyme derivatives in protein crystallography to solve the phasing problem in structure determination.[17] The first crystal structure of such a mercury derivative has only recently been reported on poplar plastocyanin, in which the copper atom was replaced by mercury.[18] Additionally, Hg EXAFS has been reported for only a few biological samples, including studies of the mercury-replaced copper proteins plastocyanin, azurin, stellacyanin, and laccase.[19] Preliminary studies have appeared on Hg_7 metallothionein that suggest sulfur ligation at an average distance of 2.40 Å.[20] Almost no structural information is available on mercury coordination for those enzymes involved specifically in mercury processing and detoxification.

In contrast to many metalloproteins, mercuric reductase does not possess a stably bound metal ion. Instead, the metal of interest is the redox substrate for the enzymic reaction, being reduced and expelled from the protein during turnover, thus complicating detailed structural studies. Our previous investigations have determined, however, that the active site of mercuric reductase can be mercurated by the addition of 1 equiv of $HgCl_2$ to the EH_2 enzyme form in a titration monitored by absorbance spectroscopy, as the Cys_{140} thiolate–FAD charge transfer is quenched;[10] the enzyme requires additional electron input from NADPH to effect mercury reduction and turnover. However, for EXAFS analysis with the aim of identifying ligands bound to Hg(II), $HgCl_2$ is not a useful titrant, as the EXAFS scattering phenomenon is highly dependent upon the atomic number of the backscattering atoms and will not readily distinguish between chlorine (e.g., $HgCl_2$) and sulfur (e.g., HgS_2–enz) ligation. We have therefore performed stoichiometric titrations of the EH_2 form of the enzyme with $Hg(CN)_2$ and $HgBr_2$, monitored by both absorbance and fluorescence spectroscopy. The displacement of cyanide or bromide ligands by enzymic thiols can then be easily discerned by EXAFS studies on the resulting metalloproteins because of the large differences in atomic number between Br, CN, and S–enzyme ligands.

In this paper we report the results of the first Hg EXAFS experiments conducted on mercuric reductase. We have studied mercurated derivatives of two forms of the Tn501 gene product: wild-type mercuric reductase (containing Cys_{135}, Cys_{140}, Cys_{558}, Cys_{559} = CCCC) and the protein, generated by site-directed mutagenesis, in which the two C-terminal cysteine residues have been changed to alanines (Cys_{135}, Cys_{140}, Ala_{558}, Ala_{559} = CCAA) and which is now essentially inactive for the reduction of Hg(II). In the mutant enzyme, which retains only two of the four possible active-site cysteines, the Hg(II) coordination is restricted to a maximum of two thiols; the wild-type enzyme has available up to four cysteines for thiol ligation to mercury. By comparing the EXAFS results for both the wild-type and mutant proteins, we proposed to determine the effect of C-terminal cysteines on the Hg(II) coordination environment in the active site of mercuric reductase.

Experimental Section

A. Protein Preparation. Wild-type and mutant mercuric reductases were purified from *Escherichia coli* W3110 *lacI*^{q} harboring plasmids pPSO1 or pMMOa558a559 as previously described[7] except for the following modifications. First, prior to Orange-A affinity chromatography, the protein was fractionated by ammonium sulfate precipitation. The mercuric reductase proteins that precipitated between 35 and 65% ammonium sulfate saturation were then resuspended in purification buffer, dialyzed against 500 volumes of buffer, and loaded onto Orange-A columns. After elution from the affinity column, the proteins were dialyzed against purification buffer (500 volumes) supplemented with 2 M KBr to remove enzyme-bound $NADP^+$. The proteins were then exchanged into purification buffer by dialysis, followed by reconstitution with excess FAD to ensure complete loading of the protein with its cofactor. Prior to use in the titrations described below, the protein samples were treated with 5 mM DTT in 100 mM sodium phosphate, pH 7.4, and exchanged into 10 mM sodium phosphate, pH 7.4, by gel filtration using a P6-D6 column (Bio-Rad) previously equilibrated in this buffer. This DTT treatment reduces the C-terminal cysteine residues, which are prone to oxidation during protein isolation.[21]

B. Generation of Mercurated Protein Samples. For the generation of mercurated protein samples, the proteins (approximately 25 mL of a 50 μM protein solution) were transferred to a 250-mL customized round-bottom flask equipped with a vacuum stopcock, a fluorescence cuvette, and a syringe port.[22] Due to the O_2-sensitive nature of the EH_2 species and its derivatives, all manipulations of these species were performed under anaerobic conditions. The enzyme solutions were made anaerobic by cycling for 1 min under vacuum (20 Torr) followed by 5 min at 1 atm of Ar(g) and repeating the process 10 times. NADH, $Hg(CN)_2$, and $HgBr_2$ solutions were degassed by a similar procedure. All degassing manipulations were carried out at 0 °C in an ice bath; all subsequent titrations were performed in water baths or instruments thermostated to 10 °C. The EH_2 form of each enzyme solution was prepared by an NADH titration whose progress was followed by absorbance and fluorescence spectroscopy.[23] These titrations were carried out over a 1-h period, followed by a 30-min equilibration time, to verify that no further spectral changes were occurring.[24] After NADH titration, the syringe was exchanged for one containing $Hg(CN)_2$ or $HgBr_2$. The EH_2 protein solution was then titrated with 1 equiv of the desired Hg(II) compound while being monitored by absorbance and fluorescence spectroscopy. These titrations required approximately 1 h and were terminated by freezing the sample at −70 °C in a dry ice/acetone bath. Mercurated protein samples were prepared by titrations with $Hg(CN)_2$ and $HgBr_2$ of both the wild-type and the Ala_{558}, Ala_{559} (CCAA) mutant mercuric reductases.[25]

(16) Scott, R. A. *Methods Enzymol.* **1985**, *117*, 414–459.
(17) McPherson, A. *Preparation and Analysis of Protein Crystals*; John Wiley and Sons: New York, 1982; pp 181–195.
(18) Church, W. B.; Guss, J. M.; Potter, J. J.; Freeman, H. C. *J. Biol. Chem.* **1986**, *261*, 234–237.
(19) Schmidt, A. M.; McMillin, D. R.; Tsang, H.-T.; Penner-Hahn, J. E. *J. Am. Chem. Soc.* **1989**, *111*, 6398–6402.
(20) Hasnain, S. S.; Diakun, G. P.; Abrahams, I.; Ross, I.; Garner, C. D.; Bremner, I.; Vasak, M. *Experientia*, Suppl. **1987**, *52*, 227–236.
(21) See ref 14.
(22) Distefano, M. Ph.D. Thesis, Massachusetts Institute of Technology, Cambridge, MA, 1989.
(23) Although NADPH is the better substrate for Hg(II) reduction, titration to the EH_2 enzyme form results in the formation of an EH_2–$NADP^+$ species that does not readily dissociate. Since the absorbance and fluorescence properties of the enzyme-bound FAD are complicated by the bound nicotinamide, NADH was used as the reductant instead. Due to the lower affinity of this cofactor for the enzyme, titration with NADH generates a simple EH_2 species with no bound NAD^+ to complicate the absorbance and fluorescence spectra. See ref 6 and: Fox, B.; Walsh, C. *J. Biol. Chem.* **1982**, *257*, 2498–2503.
(24) In previous work, the thiol titers of the E_{ox} and EH_2 forms of both the wild-type and CCAA mutant proteins were evaluated.[13,21] It was determined that the redox-active disulfide (Cys_{135} and Cys_{140}) and C-terminal cysteines (Cys_{558} and Cys_{559}) all become reduced when the wild-type enzyme is titrated to the EH_2 form with NADH, NADPH, or sodium dithionite. This occurs even when starting with protein samples in which all four cysteines are oxidized. Similarly, it was demonstrated that the redox-active disulfide of the CCAA mutant enzyme is reduced upon titration to EH_2 with the titrants listed above. Thus we are confident that the wild-type EH_2 samples described in the present work possess active sites containing four thiols, while the CCAA mutant EH_2 protein samples retain only two.
(25) In previously reported stopped-flow kinetic experiments, we examined the reactions of wild-type mercuric reductase with $Hg(CN)_2$ when excess NADPH was present. With low levels of $Hg(CN)_2$ (1–2 equiv relative to the enzyme), rapid reduction of Hg(II) is observed; when larger amounts of $Hg(CN)_2$ are used, the enzyme becomes inhibited. Since the enzyme samples examined in the present study contain low levels of $Hg(CN)_2$ (1 equiv relative to the enzyme), we have every reason to believe that these species are catalytically viable, lacking only the additional electronic input from NADPH to complete the cycle. Miller, S. M.; Massey, V.; Ballou, D. P.; Williams, C. H.; Moore, M.; Walsh, C. In *Flavins and Flavoproteins*, Proceedings of the Ninth Symposium of Flavins and Flavoproteins, 1987; Edmondson, D. E., McCormick, D. B., Eds.: Walter de Gruyter & Co.: New York, 1987; pp 29–32.

C. **Protein Sample Preparation.** After the reaction was stopped by freezing as described above, the protein samples were lyophilized at 20 mTorr for 12 h while the sample temperature was limited to −15 °C by using an ethylene glycol/dry ice bath. The lyophilized samples were vented under a N_2 atmosphere and then transferred into a glove bag equilibrated with Ar(g), where they were wetted with 100 μL of anaerobic glycerol and packed into Plexiglas sample holders previously described. The resulting samples were then frozen in liquid N_2 and stored in such for use in EXAFS experiments.

D. **Preparation of Model Samples.** $HgBr_2$, $Hg(CN)_2$, cinnabar, metacinnabar, and $HgCo(SCN)_4$ were purchased from Alfa-Ventron. $Hg(SEt)_2$ and $Hg(StBu)_2$ were synthesized by literature methods[26] and recrystallized from ethanol. The compounds were ground to powder in an agate mortar and pestle and mixed with glycerol to a final concentration of 500 mM. The mulls were loaded onto Plexiglas sample holders and frozen as above.

E. **X-ray Absorption Measurements.** X-ray absorption measurements of frozen protein samples and model compounds were conducted at the Cornell High Energy Synchrotron Source (CHESS) on the C1 beam line.[27] The synchrotron used electron–positron energies of 5.3 GeV and a storage ring injection current of 30 mA. A Si (111) double-crystal monochromator, detuned by 50% for harmonic rejection, was calibrated with a sample of liquid mercury metal at 12284 keV. Mercury L_{III}-edge EXAFS spectra were collected in the fluorescence mode by using a cryostat and Stern-Heald detector.[28] Both incident and fluorescence ionization chambers were filled with argon gas. Frozen protein samples in Plexiglas holders were prepared as described above and kept between −45 and −35 °C during data acquisition. All spectra were recorded from 12125 to 12925 eV with scan times of 25–35 min and a beam size of 1.5 × 15 mm^2. Two to three spectra of the samples containing mercury model compounds were collected. For each protein sample, 25–35 spectra were taken, yielding a total acquisition time of 10–12 h.

F. **Data Analysis.** Data analysis was performed according to the method of Teo.[29-31] The background was removed via a cubic spline function with three sections. The data were converted to k space according to $k = [8\pi[2m_e(E - E_0)/h^2]]^{1/2}$, where m_e is the electron mass. E_0 was consistently chosen as the photon energy at half-height of the absorption jump. The data were weighted by a factor of k^3 to offset attenuation of the EXAFS signal with increasing photon energy. The EXAFS signal $k^3[\chi(k)]$ vs k was truncated at 2.5 and 11 Å and then Fourier transformed and Fourier filtered between 1.4 and 2.8 Å. The best-fit distances and coordination number values were determined by fitting the Fourier filtered data in k space to the theoretical phase and amplitude function of Teo and Lee.[31] For each absorber/scatter pair, four parameters are varied in the nonlinear least-squares curve fitting: the scale factor B_j (the scale factor B_j is related to the number of neighbors N_j by the equation $B_j = S_jN_j$, where S_j is the amplitude reduction factor obtained from model compounds), the Debye–Waller factor σ_j, the distance r_j, and the threshold energy difference E_0. The refinements were based upon minimization of the unweighted sum of squares of the residuals $x^2 = \sum k_i^3[X(k)_j - Y(k)_j]^2$, where $X(k)_j$ is the experimental data and $Y(k)_j$ the calculated value of the EXAFS function.[29] The model compounds were similarly analyzed (Table I) and were used to refine bond distances and coordination numbers according to the fine adjustment based on models (FABM) method.[32] Errors in Hg–S distances and Debye–Waller factors were estimated by varying the appropriate term in the fit to the Fourier filtered data. The range required to double the goodness of fit (x^2) was taken as twice the uncertainty in the parameters.

Results

Preparation of Hg(II)–Enzyme Complexes. The EH_2 forms of wild-type (CCCC) and mutant (CCAA) mercuric reductases were titrated with 1 equiv of either $Hg(CN)_2$ or $HgBr_2$ to yield stoichiometrically mercurated enzyme complexes. The resulting absorbance and fluorescence emission spectra from titrations with $Hg(CN)_2$ are shown in Figure 1.

Scheme I. Schematic Representation of Events Occurring during Reduction of the CCAA Mutant with NADH Followed by Titration with 1 equiv of HgX_2[a]

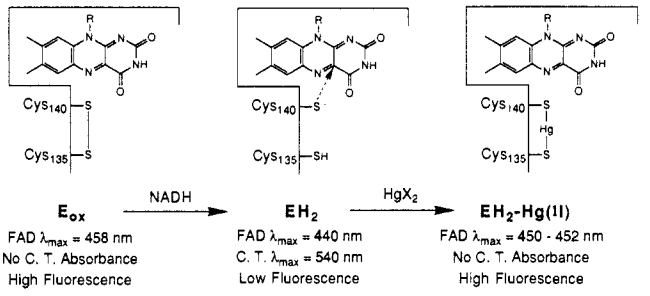

[a] The redox state of the Cys_{135}, Cys_{140} disulfide and the putative mode of Hg(II) binding are illustrated along with the spectroscopic properties of each species. The Cys_{140} thiolate–FAD charge-transfer interaction is represented by a dashed arrow.

Absorbance measurements of the wild-type complexes indicate that the active-site Cys_{140} thiolate–flavin charge-transfer absorbance is largely quenched (<11% of the EH_2 A_{540} remains) in the $Hg(CN)_2$ titration (see panel A). Similar results were obtained in the $HgBr_2$ titration (<12% of the A_{540} remains). The FAD λ_{max} values for the mercurated enzyme complexes generated by $Hg(CN)_2$ and $HgBr_2$ titration of wild type are both 456 nm. These can be compared with a λ_{max} of 456 nm for the wild-type E_{OX} form and 440 nm for EH_2. Clearly, the mercurated forms are spectrally similar to E_{OX}. (It should be pointed out that while the spectra converge to an E_{OX}-like species upon titration with Hg(II), no isosbestic points occur in the absorbance spectra of the titration mixture, suggesting that more than two species, EH_2 and EH_2–Hg(II), are present.)

Titrations of the mutant enzyme with $Hg(CN)_2$, shown in Figure 1, panel C, and with $HgBr_2$ are similar to the wild type but display some key differences. Titration with $Hg(CN)_2$ again results in almost complete quenching of the Cys_{140} thiolate–flavin charge-transfer absorbance (<1% remains); similar results are obtained in the titration with $HgBr_2$, consistent with Hg(II) ligation to at least that thiol. While the extent of CT quenching is similar in both the mutant and wild-type enzymes, the position of the FAD absorbance maximum is blue-shifted, by 4–6 nm, in the mutant protein titrated with $HgBr_2$ (λ_{max} = 452 nm) and $Hg(CN)_2$ (λ_{max} = 450 nm). This shift of EH_2–Hg(II) relative to E_{OX} is illustrated in Figure 1, panel C.

Hg(II) binding to wild-type and mutant (CCAA) mercuric reductases was also characterized by fluorescence spectroscopy, monitoring changes in the fluorescence of bound FAD. This method takes advantage of the fluorescence quenching effect of the thiolate–flavin charge-transfer complex present in the EH_2 species; as Hg(II) binds to the charge-transferring thiolate anion, fluorescence quenching is prevented. The similarities between EH_2–Hg(II) and E_{OX} are further accentuated by fluorescence data which indicates that, during Hg(II) titration, the enzyme-bound FAD fluorescence increases ca. 8-fold, to levels comparable to that of the oxidized enzyme. The actual values for the enzyme-bound FAD fluorescence of the mercurated enzyme species are 6.8 times that of free FAD for the $Hg(CN)_2$-treated sample (see Figure 1, panel B) and 7.3 times that of free FAD for the enzyme titrated with $HgBr_2$. Similar titrations of the CCAA mutant protein with $Hg(CN)_2$ yield a species possessing only 4.0 times the fluorescence of free FAD, as is shown in Figure 1, panel D. Titration of the CCAA mutant with $HgBr_2$ yields a species 3.6 times as fluorescent as free FAD. Note that the fluorescence of the oxidized forms of both the wild type and the CCAA mutant is 6.3 times that of free FAD.[14]

Thus, as illustrated above, wild-type and mutant mercuric reductases can be mercurated by titration of the two-electron-reduced, active-site dithiol-containing form, EH_2, with either $Hg(CN)_2$ or $HgBr_2$. Since the absorbance at 540 nm (the charge-transfer λ_{max}) is indicative of the amount of free EH_2

(26) Wertheim, E. *J. Am. Chem. Soc.* **1929**, *51*, 3661–3664.
(27) Batterman, B. W. In *EXAFS Spectroscopy: Techniques and Applications*; Teo, B.-K.; Joy, D. C., Eds.; Plenum Press: New York, 1981; pp 197–204.
(28) The EXAFS Co., Seattle, WA. Also see: Stern, E. A.; Heald, S. M. *Rev. Sci. Instrum.* **1979**, *50*, 1579–1582.
(29) Teo, B.-K. *EXAFS*: Basic Principles *and Data Analysis*; Springer-Verlag: New York, 1986; pp 114–181.
(30) Teo, B.-K. *Acc. Chem. Res.* **1980**, *13*, 412–419.
(31) Teo, B.-K.; Lee, P. S. *J. Am. Chem. Soc.* **1979**, *101*, 2815–2832.
(32) Teo, B.-K.; Antonio, M. R.; Averill, B. A. *J. Am. Chem. Soc.* **1983**, *105*, 3751–3762.

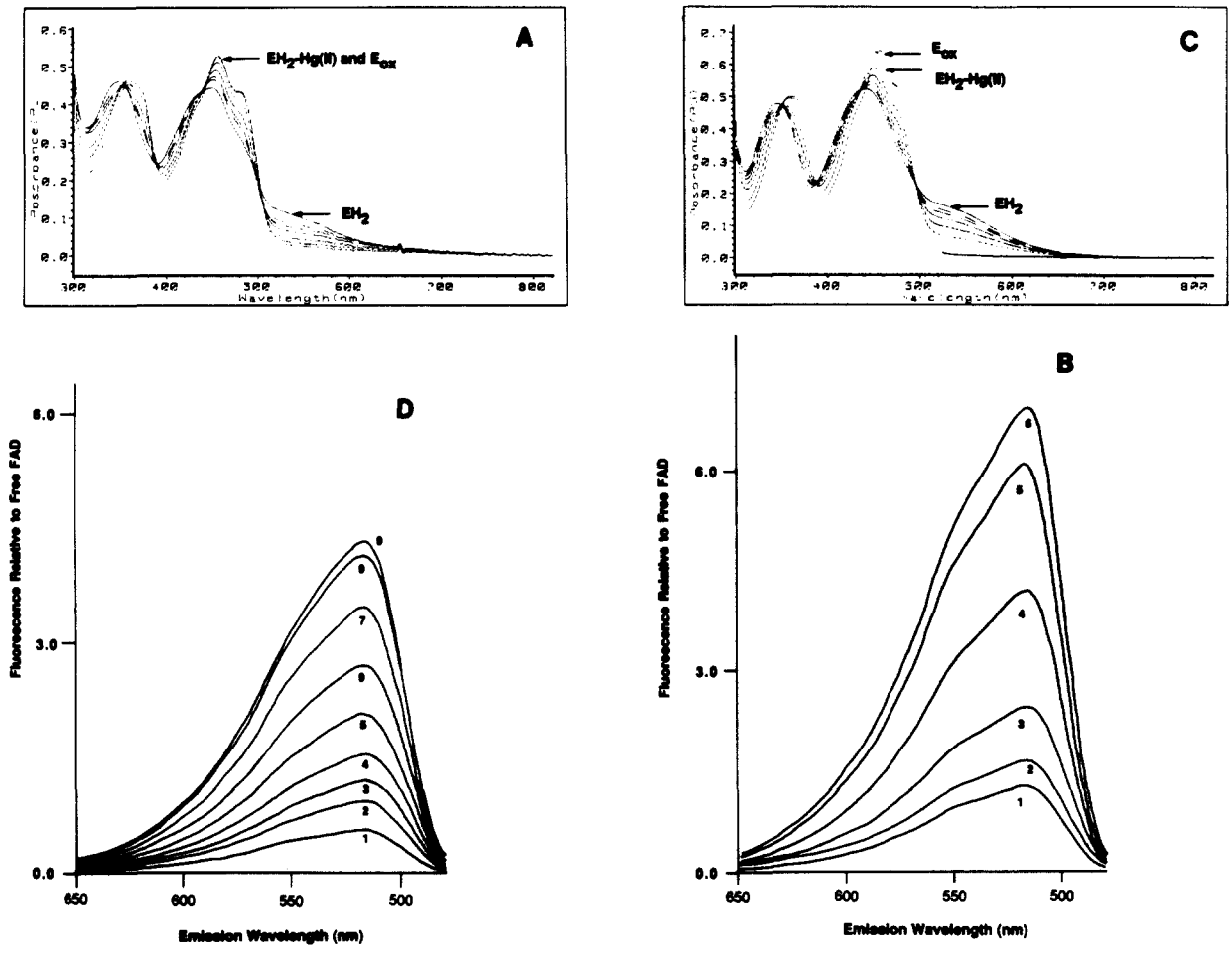

Figure 1. Absorbance and fluorescence emission spectra from titration of the wild-type and CCAA mutant mercuric reductases with $Hg(CN)_2$. (A) Absorbance spectra of wild-type mercuric reductase upon titration with $Hg(CN)_2$. The spectrum E_{OX} is the initial spectrum of the enzyme prior to NADH titration; the spectrum denoted EH_2 is that obtained after titration with NADH. The spectrum marked EH_2–Hg(II) is that of the enzyme after titration 1.04 equiv of $Hg(CN)_2$. The remaining spectra are those obtained during titration with $Hg(CN)_2$ after the addition of 0.30, 0.50, 0.70, and 0.90 equiv of Hg(II). (B) Fluorescence emission (excitation at 450 nm) spectra of wild-type mercuric reductase upon titration with $Hg(CN)_2$. (1) Spectrum of EH_2 generated by NADH titration. (2–6) Spectra after the addition of 0.30, 0.50, 0.70, 0.90, and 1.04 equiv of $Hg(CN)_2$, respectively. (C) Absorbance spectra of the CCAA mutant mercuric reductase upon titration with $Hg(CN)_2$. The spectrum E_{OX} is the initial spectrum of the enzyme prior to NADH titration; the spectrum denoted EH_2 is that obtained after titration with NADH. The spectrum marked EH_2–Hg(II) is that of the enzyme after titration with 1.00 equiv of $Hg(CN)_2$. The remaining spectra are those obtained during titration with $Hg(CN)_2$ after the addition of 0.11, 0.24, 0.38, 0.51, 0.65, 0.79, and 0.92 equiv of Hg(II). (D) Fluorescence emission (excitation at 450 nm) spectra of the CCAA mutant mercuric reductase upon titration with $Hg(CN)_2$. (1) Spectrum of EH_2 generated by NADH titration. (2–9) Spectra after the addition of 0.11, 0.24, 0.38, 0.51, 0.65, 0.79, 0.92, and 1.00 equiv of $Hg(CN)_2$, respectively.

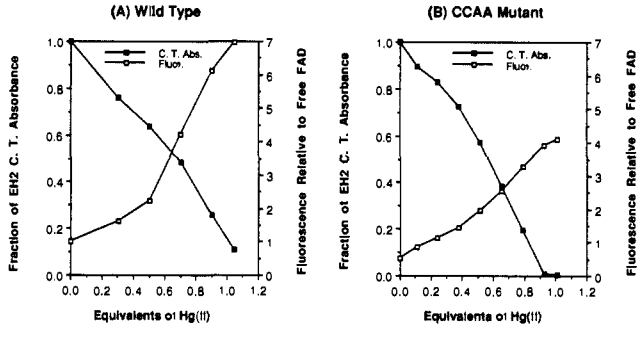

Figure 2. Charge-transfer absorbance and FAD fluorescence of samples of wild-type and CCAA mutant mercuric reductases during titrations with $Hg(CN)_2$. (A) The fraction of EH_2 charge-transfer absorbance present in a sample of wild-type mercuric reductase during titration of the EH_2 enzyme form with $Hg(CN)_2$ is shown on one y-axis of this graph. The fluorescence (excitation at 450 nm, emission at 520 nm) relative to that of the EH_2 species during the same titration is given on the other y-axis. Note that the oxidized enzyme form has no charge-transfer absorbance. (B) A graph similar to that described in (A) for a titration of the CCAA mutant enzyme with $Hg(CN)_2$.

present, the stoichiometry of Hg(II) binding to the active-site thiol (Cys_{140}) of the enzyme can be assessed by monitoring the decrease in A_{540} as Hg(II) is added. The molecular nature of these events is diagrammed in Scheme I.

The fractions of the 540-nm CT absorbance remaining during titrations of wild-type and mutant mercuric reductases with $Hg(CN)_2$ are shown in Figure 2. For wild-type enzyme, these data indicate that addition of 1 equiv of $Hg(CN)_2$ results in 89% of the Hg(II) binding to the active-site Cys_{140} thiol. By the same criterion, 99% of the Hg(II) is bound to the Cys_{140} thiol in the mutant enzyme. These results indicate that Hg(II) from $Hg(CN)_2$ and $HgBr_2$ can be readily introduced into the active site of mercuric reductases in stoichiometric quantities, as required for EXAFS experiments.

While the above data clearly indicate that Hg(II) is binding to the Cys_{140} thiol, the mercurated wild-type and mutant complexes may not be identical. Fluorescence spectroscopy during $Hg(CN)_2$ titrations of wild-type and mutant mercuric reductases (see Figure 2) demonstrates that the bound FAD coenzyme in the wild-type mercurated complex is more fluorescent (6.8 times the fluorescence of free FAD) than in the mutant EH_2–Hg(II) complex (4.0 times the fluorescence of free FAD). Additionally, the shift in the FAD absorbance λ_{max} of the mutant enzyme (see Figure 1, panel C) is in marked contrast to the unshifted FAD λ_{max} characteristic of the wild-type protein shown in Figure 1, panel A. Additionally, small differences (2–4 nm) exist in the positions of the isosbestic

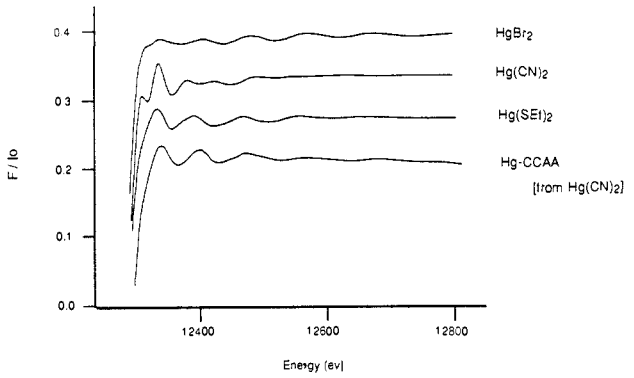

Figure 3. X-ray absorption spectra of four representative mercury compounds. The X-ray absorption spectra of the starting titrants $HgBr_2$ and $Hg(CN)_2$ are shown with the resulting mercurated enzyme derivative and a representative mercury–thiol compound, $Hg(SEt)_2$. The base-line-corrected EXAFS region is expanded for comparison.

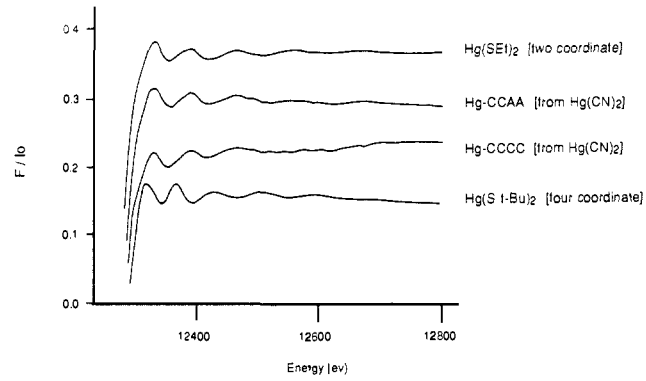

Figure 4. X-ray absorption spectra of mercury–thiol complexes. The X-ray absorption spectra of both the mercurated wild-type and mutant proteins are shown next to two model mercury–thiol complexes having two- and four-coordination, respectively. The base-line-corrected EXAFS region is expanded for comparison.

points in the wild-type and mutant titrations with Hg(II). Thus, it is possible that the wild-type and mutant mercurated complexes contain Hg(II) bound in nonidentical ways (e.g., two-coordinate vs three- or four-coordinate mercury, or different two-coordinate species).

EXAFS of Hg(II)–Enzyme Complexes. The mercury EXAFS spectrum of a representative mercurated protein sample (in this case the C-terminal double mutant CCAA) is compared to those of the starting titrants $HgBr_2$ and $Hg(CN)_2$ and of a two-coordinate mercury model thiol complex, $Hg(SEt)_2$, in Figure 3. In general, as the atomic number of the scattering atom increases, the amplitude of the EXAFS envelope moves to higher energies. Thus, the bromide ligands in $HgBr_2$ still show a substantial contribution to the EXAFS spectrum at 12.8 keV, in contrast to cyanide (in $Hg(CN)_2$), which is essentially featureless at that energy. The perdominant features of the EXAFS spectrum of $Hg(CN)_2$ occur at much lower energies; the interference pattern observed can be attributed to scattering contributions from the distant nitrogen. The near-linear arrangement of Hg–C–N gives rise to multiple scattering phenomena (discussed in detail elsewhere),[33] resulting in the clear resolution of two shells of scattering atoms (data not shown) that can be fit to carbon at 2.00 Å and nitrogen at 3.02 Å.[34]

The EXAFS spectrum of the mercurated protein sample (CCAA) clearly does not resemble that of either $Hg(CN)_2$ or $Hg(Br)_2$, indicating that a displacement of ligands about the mercury metal center has occurred. The data are similar to those of the model mercury thiol compound $Hg(SEt)_2$, suggesting that in the enzyme case mercury is now bound to sulfur ligand(s) upon complexation to the protein. In fact, Hg EXAFS spectra of both wild-type (CCCC) and CCAA mutant proteins titrated with $Hg(CN)_2$ fit to sulfur backscatters and not carbon or nitrogen. Including a second term for cyanide ligands in addition to sulfur and allowing all eight parameters to vary give the same goodness of fit as with sulfur alone; however, the resulting cyanide coordination numbers refine to zero. Alternatively, mercury–cyanide bond distances refine to >5.0 Å, indicating little evidence for direct cyanide coordination to mercury. Restricted fits using representative bond distances for Hg–CN, 2.00 ± 0.5 Å, and for Hg–S, 2.35 ± 0.5 Å, and fixed coordination numbers N = 1, 2 gave significantly poorer fits, increasing the sum of the squares of the residuals by an order of magnitude. These results indicate that

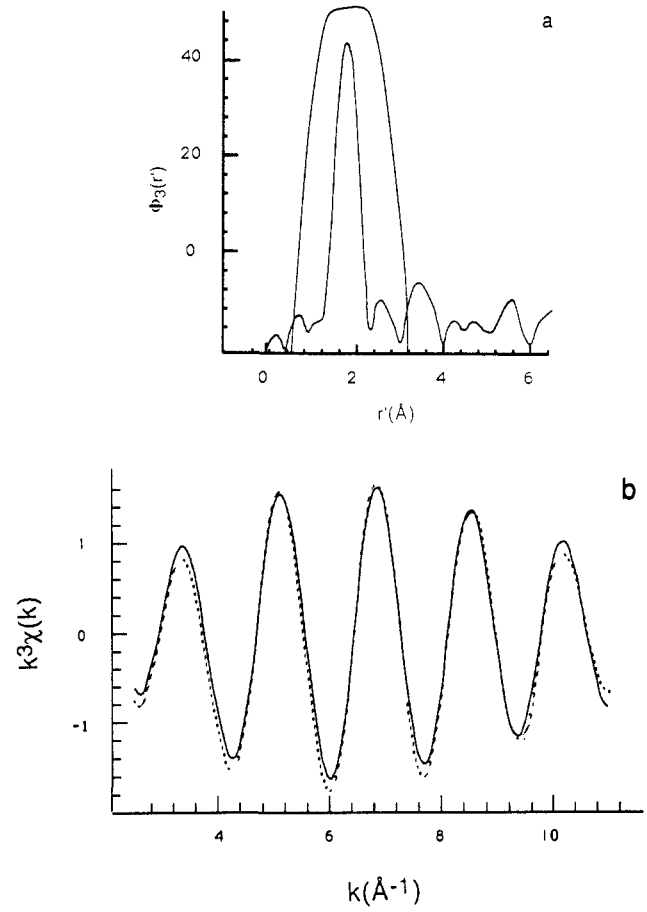

Figure 5. Fourier transform (a) and filtered (b) data of the $k^3[\chi(k)]$ vs k EXAFS spectrum from the mercury edge of Hg–CCAA [titrated with $Hg(CN)_2$]. The parabola in the Fourier transform is the window function used in Fourier filtering. The dashed line in the filtered data is the one-term Hg–S fit, yielding the parameters in Table I.

complete displacement of both ligands on Hg(II) has occurred, forming a Hg–thiol–enzyme complex. Similarly, no evidence was found for remaining bromide coordination to the mercurated enzyme samples formed from titrations with $HgBr_2$. Attempts to include bromide ligands in addition to sulfur using restricted fits such as those described above increased x^2 values by a factor of 50 over fits of the data to Hg–S distances alone.

Figure 4 compares the EXAFS spectra of both the mercurated mutant (CCAA) and native (CCCC) proteins (having Hg–S ligation) to those of two representative mercury–thiol compounds. $Hg(SEt)_2$ is typical of two-coordinate mercury, having a short, linear Hg–S distance of 2.35 Å.[35] The crystal structure of

(33) Teo, B.-K. Multiple Scattering and Bond Angle Determinations. In ref 29, pp 183–220. For a discussion of the linear Fe–C–O bond in $Na_2Fe(CO)_4$, see also: Teo, B.-K. *J. Am. Chem. Soc.* **1981**, *103*, 3990–4001.

(34) X-ray and neutron diffraction analysis of $Hg(CN)_2$ (Hvoslef, J. *Acta Chem. Scand.* **1958**, *12*, 1568–1574) reveals a Hg–C distance of 1.99 Å, a C–N distance of 1.19 Å, and an Hg–C–N angle of 173°. A long-range Hg–N interaction of 2.70 Å with nearby $Hg(CN)_2$ units was also reported, which may account for a shortening of the Hg–N distance as determined by EXAFS spectroscopy.

Table I. Summary of EXAFS Results

sample	Hg–S distance, Å ± 0.03	Debye–Waller factor, Å ± 0.02	coord. no.
$Hg(SEt)_2$	2.35	0.025	2
HgS_{red}	2.39	0.041	2
$Hg(StBu)_2$	2.55	0.059	4
HgS_{black}	2.52	0.065	4
$HgCo(SCN)_4$	2.56	0.054	4
Hg–CCAA [from $Hg(CN)_2$]	2.32	0.042	2.9
Hg–CCAA (from $HgBr_2$)	2.30	0.068	2.2
Hg–CCCC [from $Hg(CN)_2$]	2.30	0.055	2.7
Hg–CCCC (from $HgBr_2$)	2.30	0.073	2.4

$Hg(StBu)_2$ is comprised of tetrahedral four-coordinate mercury with each thiolate bridging two mercury atoms, leading to a longer average Hg–S distance of 2.62 Å.[36] The differences between the two models are clearly seen in the EXAFS spectra, where the longer Hg–S distance in four-coordinate $Hg(StBu)_2$ results in a shortening of the frequency of the Hg–S sine wave. Inspection of the spectra from the mutant and native protein samples reveals that they are quite similar and both are comparable to two-coordinate $Hg(SEt)_2$ containing the shorter Hg–S bonds.

The Fourier transform of the normalized EXAFS $k^3[\chi(k)]$ vs k and the filtered data for the CCAA protein are shown in Figure 5. The data were fit in k space to the theoretical phase and amplitude functions of Teo and Lee;[31] reasonable fits could only be obtained to sulfur, and not nitrogen (or oxygen). Restricted fits including additional sulfur ligands at longer distances significantly decreased the goodness of fit. A summary of the results for all four protein samples as well as the two-coordinate and four-coordinate mercury–sulfur model compounds used in this study is reported in Table I. In all cases a one-term mercury–sulfur scattering pair was adequate to fit the data.

EXAFS Spectra of Mercurated Enzyme Samples. Titration of the active site of either native (CCCC) or C-terminal Ala_{558}, Ala_{559} mutant (CCAA) mercuric reductase dimers by either $HgBr_2$ or $Hg(CN)_2$ results in binding of approximately one atom of mercury per active site, as followed by both absorbance and fluorescence spectroscopy. EXAFS spectroscopy of these resulting mercurated proteins clearly indicates complete displacement of the starting ligands by protein thiol (cysteine) groups, as shown in Figures 3–5. The mutant protein (CCAA) has been designed and constrained by site-directed mutagenesis to a maximum of two-thiol (Cys_{135}, Cys_{140}) coordination for active-site mercury, and the EXAFS results (Figures 4 and 5 and Table I) confirm this.

Native mercuric reductase (CCCC) contains the four cysteines (two from the active-site disulfide, 135 and 140, and two at the C-terminus, Cys_{558} and Cys_{559}) that are necessary for catalysis. Further, subunit dimerization from inactive CCAA and AACC dimers to form an active CCAA–AACC hybrid dimer indicates that these four cysteines, two from each subunit in the dimer, can assemble to reconstitute a functional, intersubunit active site. Thus, while CCAA has only the two thiols available, the wild-type CCCC mercuric reductase has available four sulfhydryl groups for possible mercury coordination. Inspection of Figure 4 instead reveals a striking similarity to both the CCAA mutant protein and the two-coordinate model $Hg(SEt)_2$. This observation is corroborated by complete analysis of the data, which is presented in Table I. All four enzyme samples from $Hg(CN)_2$ and $HgBr_2$ titration possess short (2.30–2.32 ± 0.03 Å) mercury–sulfur bonds. The coordination numbers are likewise similar (2.2–2.9) for all four proteins and consistent with two-coordination. However, such coordination numbers derived from these and other EXAFS analyses are quite sensitive to the Debye–Waller factor, which we cannot determine very precisely (Table I). Even estimating these numbers to be accurate to ±20%, there is no indication of four-coordination in the native protein samples.

Even stronger evidence for bis-thiol ligation in the mercurated enzyme samples comes from a consideration of the bond distances of model two- and four-coordinate mercury compounds. Lawton[37] and others[38] have noted that mercury–sulfur bond distances of two-coordinate mercury are typically short (2.3–2.45 Å), consistent with the data for cinnabar[39] and $Hg(SEt)_2$[35] in Table I. Other representative examples of mercury–sulfur bond distances for two-coordinate mercury include $Hg(SCH_3)_2$ (two at 2.36 Å),[40] Hg(cysteine)$_2$ (2.33 and 2.36 Å),[41] and CH_3–Hg–cysteine (2.35 Å).[42] Longer mercury–sulfur bonds of 2.45–2.65 Å are found for crystal structures of mercury in four-coordinate tetrahedral environments.[37,38] This is indeed indicated from the analyses of $Hg(StBu)_2$[36] and metaconnabarite[43] shown in Table I. Complexes of the tetrahedral anion $[Hg(SCN)_4]^{2-}$, such as $HgCo(NCS)_4$,[44] $(PPh_4)_2Hg(SCN)_4$,[45] and $[Cu(en)_2]Hg(SCN)_4$,[46] likewise possess Hg–S distances in this range; these compounds are of interest because the mercury-containing anions are discrete molecular units and are devoid of bridging sulfur ligands subject to crystal packing forces.

Consideration of the Hg–S bond distances of 2.30–2.32 ± 0.03 Å for the stoichiometrically active-site-mercurated mercuric reductases as determined by EXAFS spectroscopy most certainly argues for two-coordination, being comparable to Hg(cysteine)$_2$, slightly on the short side. Very short mercury–sulfur bonds are found in two-coordinate $Hg[S–C(NPh)–OMe]_2$ (2.32 and 2.34 Å);[47] the reported EXAFS distances within experimental error are quite reasonable. Crystal structures of two-coordinate mercury generally show weak interactions with up to four additional atoms at long distances (>3.0 Å);[37] we would not be able to observe these with EXAFS spectroscopy, as the scattering amplitudes fall off dramatically with increasing distance for light (C, N, O, and S) elements.[16] We can conclude, however, that the presence of the two additional C-terminal cysteines in the active site of native mercuric reductase does not perturb the coordination geometry of mercury to a four-coordinate tetrahedral arrangement upon titration with HgX_2. It is possible that these cysteines may replace H_2O ligands or other protein residues to provide weak interactions with mercury at long distances to fill the coordination sphere.

Discussion

The use of EXAFS spectroscopy on metalloproteins engineered by site-directed mutagenesis couples two powerful techniques for the determination of the metal coordination environment and subsequent probing of specific metal–ligand interactions with targeted amino acids on the protein backbone. The present study focuses on two variants of mercuric reductase: the wild type, containing four cysteine residues at the active site, and the mutant (Cys_{135}, Cys_{140}, Ala_{558}, Ala_{559}), constrained to enforce only bis-

(35) This distance is determined from the EXAFS analysis and is reported in Table I. In fact, the reported Hg–S distance of 2.45 Å from the crystal structure determination (Bradley, D. C.; Kunchur, N. R. *Can. J. Chem.* **1965**, *43*, 2786–2792) is curiously long for a two-coordinate mercury–thiol complex (vide infra).

(36) Kunchur, N. R. *Nature* **1964**, *204*, 468–469. The crystal structure of four-coordinate mercury in $Hg(StBu)_2$ contains Hg–S distances of 2 × 2.66 Å and 2 × 2.59 Å.

(37) Lawton, S. L. *Inorg. Chem.* **1971**, *10*, 328–335.

(38) Levason, W.; McAuliffe, C. A. In *The Chemistry of Mercury*; McAuliffe, C. A., Ed.; The MacMillan Company of Canada Ltd.: Toronto, 1979; pp 49–115.

(39) The crystal structure of cinnabar contains two Hg–S bonds at a distance of 2.36 Å. Aurivillius, K. L. *Acta Chem. Scand.* **1950**, *4*, 1413–1436.

(40) Bradley, D. C.; Kunchur, N. R. *J. Chem. Phys.* **1964**, *40*, 2258–2261.

(41) Taylor, N. J.; Carthy, A. J. *J. Am. Chem. Soc.* **1977**, *99*, 6143–6145.

(42) Taylor, N. J.; Wong, Y. S.; Chieh, P. C.; Carthy, A. J. *J. Chem. Soc., Dalton Trans.* **1975**, 438–442.

(43) The crystal structure determination of metacinnabarite reveals four Hg–S bonds of 2.54 Å. Aurivillius, K. L. *Acta Chem. Scand.* **1964**, *18*, 1552–1553.

(44) Udupa, M. R.; Krebs, B. *Inorg. Chim. Acta* **1980**, *42*, 37–41. The X-ray structure of $Hg(SCN)_4Co(DMF)_2$ contains four Hg–S bonds ranging from 2.50 to 2.56 Å, with an average distance of 2.52 Å.

(45) Sakhri, P. A.; Beauchamp, A. L. *Acta Crystallogr.* **1975**, *B31*, 409. X-ray analysis indicates four Hg–SCN bonds ranging from 2.49 to 2.58 Å, with an average distance of 2.53 Å.

(46) Scouloudi, H. *Acta Crystallogr.* **1953**, *6*, 651–657. X-ray analysis indicates that the mercury atom is surrounded by four SCN groups at distances ranging from 2.49 to 2.61 Å, with an average distance of 2.55 Å.

(47) McEwen, R. S.; Sim, G. A. *J. Chem. Soc. A* **1967**, 1552–1558.

Scheme II. Mutant and Widl-Type Hg(II) Coordination As Determined by EXAFS[a]

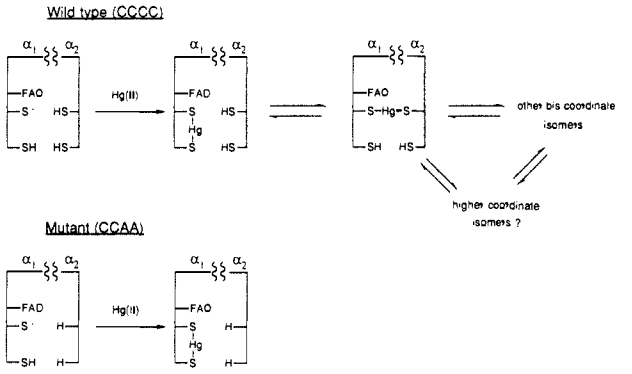

[a] The active sites of the CCAA mutant and wild-type mercuric reductases are shown schematically, along with their proposed modes of Hg(II) ligation. The intersubunit nature of the active site is illustrated by wavy lines separating the two subunits, α_1 and α_2.

ligation of Hg(II). Despite the wide difference in catalytic ability of the two proteins, the mutant being 3 orders of magnitude slower in effecting Hg(II) reduction, the coordination spheres of the mercurated proteins are strikingly similar, as determined by EXAFS spectroscopy. In each case, a two-coordinate mercury–thiolate complex is formed, with active-site cysteines having a Hg–S distance of 2.31 Å. No evidence can be found for coordination by all four active-site cysteines to Hg(II) in the wild-type mercuric reductase. These findings are in accord with the observation that most mercury–thiol complexes combine with a stoichiometry of 1:2. Tetrahedral four-coordination may be adopted in crystal structures of such adducts by bridging thiolate ligands. However, monomeric three- and four-coordinate complexes of mercury with sulfur ligands are uncommon, complexes of the pseudo-halide SCN, e.g., $Hg(SCN)_4^{2-}$, being exceptions.

$Hg(SR)_3$ (R = cysteine, glutathione, penicillamine) complexes have been implicated as intermediates in the rapid exchange of $Hg(SR)_2$ with excess thiol as studied by ^{13}C NMR.[48] Such complexes were estimated to comprise a significant fraction of the total mercuric ion in solutions having a thiol to Hg(II) ratio greater than 2:1 and at pH >5. The salts $(Et_4N)[Hg(SR)_3]$, where R = Me or tBu, and $[(Ph_3N)_2N][Hg(StBu)_3]$ have been prepared;[49] vibrational spectroscopy indicates that the $Hg(StBu)_3^-$ ion is trigonal pyramidal and $Hg(SMe)_3^-$ is multimeric in the solid state. $[N(Bu)_4]^+[Hg(SPh)_3]^-$[50] and $[N(Me)_4]^{2+}[Hg(SC_6H_4Cl)_4]^{2-}$[51] provide the only two examples in the rare class of three- and four-coordinate monomeric Hg(II)–thiolate complexes whose structures have been determined. Thus a possible interpretation of our results on mercuric reductase is that only the more common two-coordinate Hg–thiol complexes are present during the catalytic cycle of mercury reduction. In this case, the enzyme might use more than two enzyme-derived thiols in a mechanism that requires isomerization of one bis-coordinate Hg(II) species [e.g., $Hg(Cys_{558}, Cys_{559})$] to a second bis-coordinate species [e.g., $Hg(Cys_{135}, Cys_{140})$]. In this mechanism, the C-terminal cysteine residues, Cys_{558} and Cys_{559}, would be required either to ensure the correct positioning of the metal ion in the active site of mercuric reductase for subsequent reduction by $FADH_2$ or to shuttle the Hg(II) into the active-site thiol pair (see Scheme II).

An alternative explanation suggests that a three- or four-coordinate $Hg(Cys)_n$ complex is essential for subsequent reduction of mercury but that such a species occurs as a short-lived, higher energy intermediate or a transition state on the reaction coordinate. Thus the EXAFS experiments characterize the heavily populated two-coordinate ground state of mercuric reductase and would not detect a small fraction of tris- or tetrakis-coordinated mercury, which may be the productive ligation complexes for catalysis. Or, the higher coordinate Hg(II)–mercuric reductase species may form only after the input of reducing equivalents from cosubstrate NADPH, required for mercury turnover, and we observe the enzyme in a two-coordinate state, early on the pathway to mercury reduction.

A key question raised by the present findings is whether the four cysteines required for catalysis in native mercuric reductase are all sterically accessible (in a intra- or intersubunit active site) to be able to provide three- or four-coordination about a transition-metal ion. One approach to this problem is to probe for metal-based transition-state analogues of mercuric reductase, that is, transition metals (such as cadmium[52]) with a strong affinity for thiol ligation but a greater propensity than mercury for four-coordination. Biophysical studies similar to the ones presented here on both wild-type and CCAA mutant enzymes may provide additional information as to the coordination chemistry of mercuric reductase; these experiments are underway in our laboratories.

Acknowledgment. This work was supported in part by NIH Grant GM 21653. We are indebted to Dr. Melissa J. Moore for a generous gift of plasmid pMMOa558a559. We thank the staff at CHESS for assistance with the experimental apparatus used in data acquisition.

(48) Cheesman, B. V.; Arnold, A. P.; Rabenstein, D. L. *J. Am. Chem. Soc.* **1988**, *110*, 6359–6364.
(49) Bowmaker, G. A.; Dance, I. G.; Dobson, B. C.; Rogers, D. A. *Aust. J. Chem.* **1984**, *37*, 1607–1618.
(50) Christou, G.; Folting, K.; Huffman, J. C. *Polyhedron* **1984**, *3*, 1247–1253.
(51) Choudhury, S.; Dance, I. G.; Guerney, P. J.; Rae, A. D. *Inorg. Chim. Acta* **1983**, *70*, 227–230.
(52) Such $Cd(SR)_4^{2-}$ compounds have been characterized. See, for example: Swenson, D.; Baenziger, N. C.; Coucouvanis, D. *J. Am. Chem. Soc.* **1978**, *100*, 1932–1934. See also: Coucouvanis, D.; Murphy, C. N.; Simhon, E.; Stemple, P.; Dragnjac, M. *Inorg. Synth.* **1985**, *22*, 23–29.